2021 43rd Annual International Conference of the
IEEE Engineering in Medicine & Biology Society (EMBC)
Oct 31 - Nov 4, 2021. Virtual Conference

Effect of Modulating fMRI Time-Series on Fluid Ability and Fluid Intelligence for Healthy Humans

Sai Sanjay Balaji, *Student member*, *IEEE*; Bhaskar Sen, *Member*, *IEEE*; and Keshab K. Parhi, *Fellow*, *IEEE*

***Abstract*— This paper investigates the effect of filtering (or modulating) the functional magnetic resonance imaging (fMRI) time-series on intelligence metrics predicted using dynamic functional connectivity (dFC). Thirteen brain regions that have highest correlation with intelligence are selected and their corresponding time-series are filtered. Using filtered time-series, the modified intelligence metrics are predicted. This experiment investigates whether modulating the time-series of one or two regions of the brain will increase or decrease the fluid ability and fluid intelligence among healthy humans. Two sets of experiments are performed. In the first case, each of the thirteen regions is separately filtered using four different digital filters with passbands: i) 0 - 0.25π, ii) 0.25π - 0.5π, iii) 0.5π - 0.75π, and iv) 0.75π – π, respectively. In the second case, two of the thirteen regions are filtered simultaneously using a low-pass filter of passband 0 - 0.25π. In both cases, the predicted intelligence declined for 45-65% of the subjects after filtering in comparison with the ground truths. In the first case, the low-pass filtering process had the highest predicted intelligence among the four filters. In the second case, it was noticed that the filtering of two regions simultaneously resulted in a higher prediction of intelligence for over 80% of the subjects compared to low-pass filtering of a single region.**

I. Introduction

Recent studies have shown that deep brain stimulation (DBS) is effective in treating various neurological and psychiatric conditions such as treatment-resistant depression [1] and Parkinson's disease [2], [3]. It has been believed that brain stimulation can increase human intelligence. However, this has never been confirmed because an experiment to test the hypothesis on healthy humans poses serious risks and side effects. We attempt to partly answer this question by modulating the time-series of functional magnetic resonance imaging (fMRI) signals of a healthy human brain at one or two regions of the brain. The filtering of the fMRI time-series is assumed to capture the effect of brain stimulation. This may not represent the true stimulation effect of a DBS device on the fMRI time-series; nevertheless, this may lead to some understanding of effect of modulating time-series on human intelligence in healthy humans.

The statistical interdependence between the regions of the brain that share functional properties is referred to as functional connectivity and the change in this functional connectivity over time is termed as *dynamic* Functional Connectivity (dFC) [4]. In prior work [5], we showed that dFC can be used to predict intelligence metrics such as fluid ability and fluid intelligence with a smaller mean square error compared to other methods such as partial least square, correlation, network features, node entropy and edge entropy. It also identified statistically significant spatial components that correlate with intelligence metrics. Four types of digital filtering operations are performed for selected brain regions that correlate with intelligence to understand the effect of time-series modulation on intelligence. Filtering of two regions simultaneously is also performed to compare the predicted intelligence against filtering the time-series of a single region.

In particular, the contributions of the paper are as follows. First, we analyze the predicted intelligence metrics for the modulated fMRI time-series with ground truth. Our goal is to identify the possibility of enhancing human intelligence by stimulation of suitable brain regions. Moreover, our experimental result also enables us to identify subjects for whom modulation would be beneficial.

The remainder of the paper is organized as follows. Section II briefly describes the data, pre-processing of fMRI and the digital filtering methods. Section III describes the experimental results.

II. Experimental Setup

The data and pre-processing steps are described in [5] and are summarized in subsections II-A, II-B and II-C. Filtering of fMRI time-series is described in Subsection II-D.

A. Data

The Q2 release of Human Connectome Project (HCP) Database [6], [7] consisting of resting-state and task fMRI data of 475 subjects is used for the experiment. The task data contains the fMRI data when the subjects performed the following seven tasks: a) Emotion, b) Gambling, c) Language, d) Motor, e) Relational, f) Social, and g) Working Memory. The collection of the data was approved by the Institutional Review Board at the University of Minnesota.

The intelligence metrics are modeled by two target values:

- Fluid Intelligence: It is estimated using the Penns Progressive Matrices (PMAT) [8], which is a shortened version of Ravens Progressive Matrices. This test had a mean of 16.09, standard deviation of 5.98 and range of 4-24. The participants in this test were given an incomplete puzzle with a visual pattern and they filled the missing piece from a given set of pieces.
- Fluid Ability: This metric is impacted by the age as it changes from childhood to adolescence and reduces thereafter upon aging. It is characterized using *The Pattern Comparison* test where the subjects were asked

This research was supported in part by the National Science Foundation under grant number CCF-1954749.

S. Balaji, B. Sen and K. K. Parhi are with the Department of Electrical and Computer Engineering, University of Minnesota, Minneapolis, MN 55455, USA (email: balaj037@umn.edu, senxx056@umn.edu and parhi@umn.edu).

to identify if a given set of images are the same. The scores were normalized to obtain an age-adjusted scale. This test result has a range of 47-150.

B. Pre-processing

The fMRI data are processed using the HCP pipeline tool followed by spatial smoothing and generation of activation maps. Considering the Freesurfer cortical parcellation atlas [9], the mean time-series values of voxels for each subject were then extracted for the 85 regions of interest. The one-shot absolute Pearson's correlation values are extracted for each subject from the mean time-series for analyzing the static connectivity. The time-series data for each subject were then divided into multiple sliding windows of varying strides. As observed in [5], a stride value of 5 yielded best results in intelligence prediction. The pairwise absolute Pearson's correlation were calculated for each subject and each time window for the 85 regions.

As the values of correlation coefficient are bidirectional, it is sufficient to consider one set of values for each pair of regions. From this we get $\binom{85}{2} = 3570$ edge correlation values, which can be considered as a 3570×1 vector. The correlation vectors extracted for each window are stacked to form a dynamic functional connectivity matrix (size $3570 \times T$ where T depends on the sliding window stride). Dynamic functional connectivity matrices were then concatenated to form a 3-dimensional tensor of size $3570 \times T \times 475$. For the given HCP time-series data and a stride value of 5, $T = 26$.

C. Tensor Decomposition

PARAFAC decomposition [10] of the tensor (obtained by concatenating the dynamic connectivity matrix of the 475 subjects) was performed, which can be summarized as follows. The three-dimensional tensor $\mathcal{X}$ of size $I_1 \times I_2 \times I_3$ can be expressed using smaller rank-1 tensors as:

$$\mathcal{X}_{I_1,I_2,I_3} = \sum_{f=1}^{F} a_f \circ b_f \circ c_f \tag{1}$$

where $\circ$ denotes the outer product. From this, the factor matrices **A**, **B** and **C** of respective size $I_1 \times F, I_2 \times F$ and $I_3 \times F$ are obtained whose corresponding columns are the associated factors a_f, b_f and c_f. The matrix **A** corresponds to the estimated connectivity maps, **B** corresponds to the time variation and **C** corresponds to the subject-wise weight.

Using Pearson's correlation, thirteen regions of significance are identified in [5]. Matrix **C** was used for this purpose and the top 5% of the connecting edges were identified from the corresponding columns of **A**.

D. Digital Filtering

Having identified the thirteen regions in the brain that have high correlation with intelligence, the mean time-series data from these regions of each subject are filtered using a digital filter one region at a time. For this, four separate filtering operations are performed on each of the thirteen regions. The normalized passband frequency range of each filter is as follows: i) 0 - 0.25π, ii) 0.25π - 0.5π, iii) 0.5π - 0.75π, and iv) 0.75π – π. The filtered time-series in each case is used to construct the dynamic connectivity tensor. The decomposition of the tensor using the N-way toolbox [11] is further constrained to retain the same value for the matrix **A** that corresponds to the connectivity, as the spatial connectivity of the 85 regions remain the same. Thus, new subject-wise weight matrix $\mathbf{C}_{new}$ is obtained for each filtered time-series.

With the weight matrix corresponding to the original time-series data (**C**) used as features and the intelligence metrics (fluid intelligence and fluid ability) as target values, a bag of decision trees is used to predict the new values of the fluid intelligence and fluid ability for the weight matrix corresponding to the filtered time-series $\mathbf{C}_{new}$. This is then compared with the original value and the prediction of unfiltered data obtained by using the method described in [5].

After observing that the low-pass filtering leads to the highest predicted intelligence, we filter two of the thirteen regions simultaneously using a low-pass digital filter using passband 0 - 0.25π and repeat the process of predicting fluid intelligence and fluid ability for each of the 78 such combinations. The findings of both the set of experiments are described in the next section.

III. Results

A. Filtering of a Single Region

Tables I and II show the percentage of users (among the 475 subjects) whose intelligence metrics increased upon filtering of the fMRI time-series. It is observed that the predicted value of the intelligence metrics is less after filtering than the original value (the ground truth) or the predicted value of the unfiltered data for about 45% - 65% of the subjects, depending on the region filtered and the type of filter. The change in fluid intelligence varied from -10 to +15 and that of fluid ability from -55 to +60. However, the direction of change remains mostly the same for a given subject and the magnitude varied based on the region filtered.

It is seen that filtering all the significant regions via low-pass filter led to the highest predicted intelligence metric when compared with other filters (though this was less than ground truth for many). Also, the three-dimensional tensor obtained by stacking the filtered dFC matrix for the 475 subjects were mostly similar for the filters with passband range 0.5π - 0.75π and 0.75π – π.

B. Simultaneous Low-Pass Filtering of Two Regions

Figures 1 and 2 show the relative percentage of humans for whom the predicted intelligence metrics are greater than ground truth among all possible 78 combinations for fluid intelligence and fluid ability, respectively.

From the figures, the combinations Accumbens(L) and Entorhinal(L); and Entorhinal(L) and Entorhinal(R) yielded the highest predicted value for fluid intelligence. The combinations of Amygdala(R) and Entorhinal(L); and Entorhinal(L) and Lateral Orbitofrontal(R) yielded the highest predicted value for fluid ability.

TABLE I: Percent of subjects for whom predicted value of fluid intelligence after filtering is greater than the ground truth

Region	LPF	BPF-1	BPF-2	HPF
Lateral Orbitofrontal (L)	44.84	40.42	39.37	39.58
Cuneus (L)	44.42	44.42	43.79	44.00
Rostral Anterior Cingulate (L)	46.74	46.53	46.53	45.89
Pars Orbitalis (L)	43.58	40.42	40.42	40.42
Accumbens (L)	44.84	47.37	47.16	48.00
Entorhinal (L)	42.32	46.95	47.16	46.95
Caudate (L)	45.26	46.32	46.32	45.26
Caudal Anterior Cingulate (R)	43.79	41.68	41.47	41.68
Pars Opercularis (R)	44.63	43.57	44.00	44.42
Amygdala (R)	45.47	43.58	43.37	43.58
Putamen (R)	44.84	46.53	47.58	47.37
Entorhinal (R)	45.05	40.21	40.42	40.63
Lateral Orbitofrontal (R)	45.05	41.26	41.05	40.42

TABLE II: Percent of subjects for whom predicted value of fluid ability after filtering is greater than the ground truth

Region	LPF	BPF-1	BPF-2	HPF
Lateral Orbitofrontal (L)	49.26	47.79	47.58	48.21
Cuneus (L)	48.63	39.16	38.95	39.79
Rostral Anterior Cingulate (L)	47.79	40.63	39.58	39.16
Pars Orbitalis (L)	48.84	37.89	36.63	37.05
Accumbens (L)	47.79	51.79	52.00	52.21
Entorhinal (L)	48.00	36.63	34.53	34.10
Caudate (L)	49.89	51.16	50.74	50.32
Caudal Anterior Cingulate (R)	50.32	46.74	46.53	46.32
Pars Opercularis (R)	47.58	46.11	45.47	45.47
Amygdala (R)	52.63	50.11	49.89	49.68
Putamen (R)	46.95	44.42	43.58	43.37
Entorhinal (R)	49.47	38.32	38.11	37.89
Lateral Orbitofrontal (R)	51.16	55.58	54.95	55.37

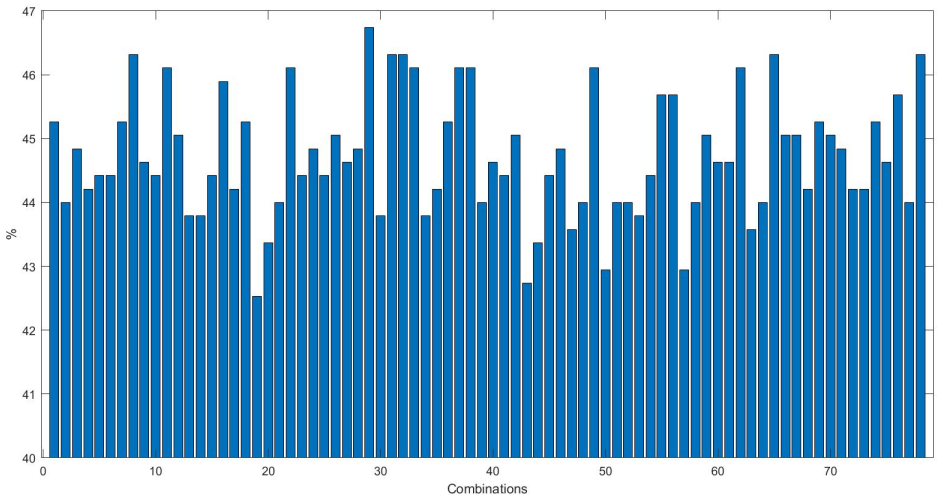

Fig. 1: Percentage of subjects with predicted fluid intelligence greater than the ground truth for the 78 possible combinations of low-pass filtering two of the thirteen regions simultaneously.

Table III illustrates the number of subjects for whom the predicted fluid intelligence and fluid ability are greater if two regions, Amygdala(R) and Entorhinal(L), are low-pass filtered simultaneously than low-pass filtering of either Amygdala(R) or Entorhinal(L). When these two regions are together filtered using a low-pass filter, the predicted intelligence metric is higher than if either of these regions is individually filtered for 427 subjects (89.89%) with respect to fluid intelligence and for 382 subjects (80.42%) for fluid ability (see Table III). These predicted values are independent of the ground truth values and of the predicted intelligence metrics at base line (without any filtering).

IV. Conclusion

This paper summarizes the effects of common digital filtering of fMRI time-series on the predicted intelligence metrics. Dynamic functional connectivity of human brain's

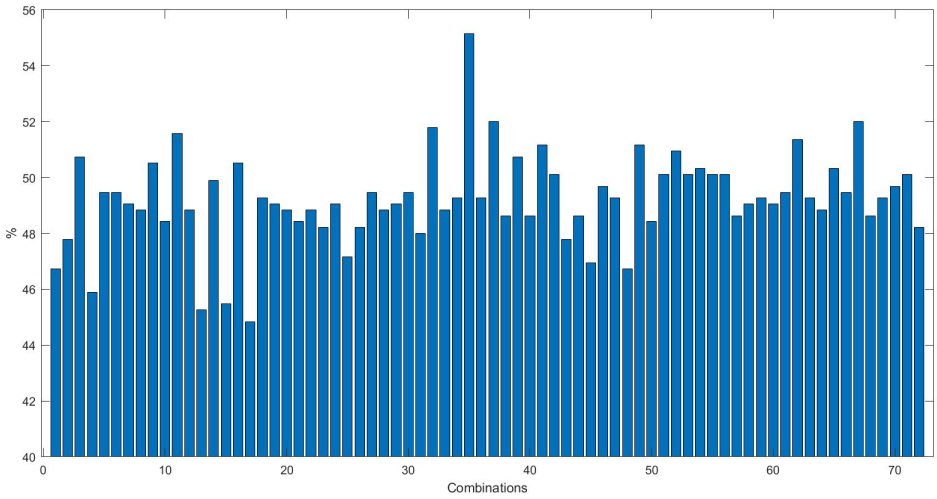

Fig. 2: Percentage of subjects with predicted fluid ability greater than the ground truth for the 78 possible combinations of low-pass filtering two of the thirteen regions simultaneously.

TABLE III: Number of subjects for whom predicted fluid intelligence and fluid ability improve after low-pass filtering of one or two regions

Brain region	Fluid Intelligence		Fluid Ability	
	# of subjects	% of subjects	# of subjects	% of subjects
Entorhinal (L)	22	4.64	43	9.01
Amygdala (R)	26	5.47	50	10.52
Combination	427	89.89	382	80.47

fMRI data can be devised as a tensor decomposition problem and the obtained weight matrix is a good feature for predicting intelligence [5]. Using this, significant regions in the brain correlating with intelligence were identified. In this experiment, we observe the change in prediction by modulating the time-series data of these significant regions through different digital filters individually, and low-pass filtering of two regions simultaneously.

The paper has demystified the myth that brain stimulation can always increase intelligence metrics of a healthy human. Using filtered time-series as a primitive form of neuromodulation and prediction based on dynamic functional connectivity, it is shown that the intelligence metrics increase for about less than half the people. Future work will be directed towards identification of features that can help in classifying if the modulation is beneficial or detrimental to the subject in terms of intelligence metrics, and experimenting the filtering operations with more than two regions at the same time. Biological interpretation of change in intelligence due to filtering of time-series needs to be investigated.

REFERENCES

[1] H. S. Mayberg, A. M. Lozano, V. Voon, H. E. McNeely, D. Seminowicz, C. Hamani, J. M. Schwalb, and S. H. Kennedy, "Deep brain stimulation for treatment-resistant depression," *Neuron*, vol. 45, no. 5, pp. 651–660, 2005.

[2] A. Stefani, A. M. Lozano, A. Peppe, P. Stanzione, S. Galati, D. Tropepi, M. Pierantozzi, L. Brusa, E. Scarnati, and P. Mazzone, "Bilateral deep brain stimulation of the pedunculopontine and subthalamic nuclei in severe Parkinson's disease," *Brain*, vol. 130, no. 6, pp. 1596–1607, 2007.

[3] J. L. Vitek, R. Jain, L. Chen, A. I. Tröster, L. E. Schrock, P. A. House, M. L. Giroux, A. O. Hebb, S. M. Farris, D. M. Whiting *et al.*, "Subthalamic nucleus deep brain stimulation with a multiple independent constant current-controlled device in Parkinson's disease (INTREPID): a multicentre, double-blind, randomised, sham-controlled study," *The Lancet Neurology*, vol. 19, no. 6, pp. 491–501, 2020.

[4] M. G. Preti, T. A. Bolton, and D. Van De Ville, "The dynamic functional connectome: State-of-the-art and perspectives," *Neuroimage*, vol. 160, pp. 41–54, 2017.

[5] B. Sen and K. K. Parhi, "Predicting Biological Gender and Intelligence From fMRI via Dynamic Functional Connectivity," *IEEE Transactions on Biomedical Engineering*, vol. 68, no. 3, pp. 815–825, March 2021.

[6] D. C. Van Essen, S. M. Smith, D. M. Barch, T. E. Behrens, E. Yacoub, K. Ugurbil *et al.*, "The WU-Minn Human Connectome Project: an overview," *Neuroimage*, vol. 80, pp. 62–79, 2013.

[7] D. C. Van Essen, K. Ugurbil, E. Auerbach, D. Barch, T. Behrens, R. Bucholz, A. Chang, L. Chen, M. Corbetta, S. W. Curtiss *et al.*, "The Human Connectome Project: a data acquisition perspective," *Neuroimage*, vol. 62, no. 4, pp. 2222–2231, 2012.

[8] W. B. Bilker, J. A. Hansen, C. M. Brensinger, J. Richard, R. E. Gur, and R. C. Gur, "Development of abbreviated nine-item forms of the Raven's standard progressive matrices test," *Assessment*, vol. 19, no. 3, pp. 354–369, 2012.

[9] R. S. Desikan, F. Ségonne, B. Fischl, B. T. Quinn, B. C. Dickerson, D. Blacker, R. L. Buckner, A. M. Dale, R. P. Maguire, B. T. Hyman *et al.*, "An automated labeling system for subdividing the human cerebral cortex on MRI scans into gyral based regions of interest," *Neuroimage*, vol. 31, no. 3, pp. 968–980, 2006.

[10] N. D. Sidiropoulos, L. De Lathauwer, X. Fu, K. Huang, E. E. Papalexakis, and C. Faloutsos, "Tensor decomposition for signal processing and machine learning," *IEEE Transactions on Signal Processing*, vol. 65, no. 13, pp. 3551–3582, 2017.

[11] C. A. Andersson and R. Bro, "The N-way toolbox for MATLAB," *Chemometrics and intelligent laboratory systems*, vol. 52, no. 1, pp. 1–4, 2000.